Biometals (2020) 33:87–95
https://doi.org/10.1007/s10534-020-00233-5

Iron chelation by deferiprone does not rescue the Niemann-Pick Disease Type C1 mouse model

Ya Hui Hung · Amit Lotan · Shlomo Yeshurun · Anna Schroeder · Ashley I. Bush

Received: 2 February 2020 / Accepted: 19 February 2020 / Published online: 25 February 2020

Abstract Niemann-Pick Disease Type C (NP-C) is a fatal lysosomal storage disorder with progressive neurodegeneration. In addition to the characteristic cholesterol and lipid overload phenotype, we previously found that altered metal homeostasis is also a pathological feature. Increased brain iron in the *Npc1*$^{-/-}$ mouse model of NP-C may potentially contribute to neurodegeneration, similar to neurodegenerative diseases such as Alzheimer's and Parkinson's diseases. Deferiprone (DFP) is a brain penetrating iron chelator that has demonstrated effectiveness in preventing neurological deterioration in Parkinson's disease clinical trials. Therefore, we hypothesized that DFP treatment, targeting brain iron overload, may have therapeutic benefits for NP-C. *Npc1*$^{-/-}$ mice were assigned to four experimental groups: (1) pre-symptomatic (P15) + 75 mg/kg DFP; (2) pre-symptomatic (P15) + 150 mg/kg DFP; (3) symptomatic (P49) + 75 mg/kg DFP; (4) symptomatic (P49) + 150 mg/kg DFP. Our study found that in *Npc1*$^{-/-}$ mice, DFP treatment did not offer any improvement over the expected disease trajectory and median lifespan. Moreover, earlier treatment and higher dose of DFP resulted in adverse effects on body weight and onset of ataxia. The outcome of our study indicated that, despite increased brain iron, *Npc1*$^{-/-}$ mice were vulnerable to pharmacological iron depletion, especially in early life. Therefore, based on the current model, iron chelation therapy is not a suitable treatment option for NP-C.

Keywords NPC1 · Niemann-Pick Disease Type C · Npc1 mouse model · Deferiprone · Iron

Ya Hui Hung and Amit Lotan have contributed equally to this work.

Y. H. Hung · A. Lotan · S. Yeshurun · A. Schroeder · A. I. Bush (✉)
Oxidation Biology Unit, Melbourne Dementia Research Centre, The Florey Institute of Neuroscience and Mental Health and The University of Melbourne, Melbourne, VIC 3052, Australia
e-mail: ashley.bush@florey.edu.au

A. Lotan
Department of Psychiatry and the Biological Psychiatry Laboratory, Hadassah Hebrew University Medical Center, Jerusalem 91120, Israel

Present Address:
A. Schroeder
Behavioural Neuroscience Laboratory, Department of Psychiatry, Monash University, Clayton, VIC 3168, Australia

Introduction

Niemann-Pick Disease Type C (NP-C) is a fatal lysosomal storage disorder affecting 1:90,000 live births (Wassif et al. 2016). NP-C is further classified as Type C1 (NP-C1; OMIM 257220) or Type C2 (NP-

C2; OMIM 607625), based on pathogenic mutations in the *NPC1* or *NPC2* genes, respectively (Carstea et al. 1997; Naureckiene et al. 2000). NP-C1 is the predominant subtype affecting about 95% of the patient population (Patterson et al. 2013). Emerging structural studies implicate NPC1 and NPC2 proteins, localized to late endosomes and lysosomes, in the transport and intracellular mobilization of cholesterol and sterols (Elghobashi-Meinhardt 2019; Hodoscek and Elghobashi-Meinhardt 2018; Gong et al. 2016; Li et al. 2017; Pfeffer 2019; Xu et al. 2007). The loss-of-function NPC1 and/or NPC2 mutant proteins block cholesterol egress from lysosomes, resulting in an excessive build-up of lysosomal cholesterol. Consequently, toxic cholesterol accumulation results in cellular and organ damage. NP-C patients present with heterogeneous clinical symptoms that include hepatosplenomegaly, cerebellar ataxia, dysarthria, dysphagia, schizophrenia-like psychosis and dementia due to progressive neurodegeneration affecting brain regions that include the cerebellum, basal ganglia, brain stem, corpus callosum, thalamus and hippocampus (Rego et al. 2019). The age of disease onset spans a wide spectrum, from in utero to late life, and typically, inversely correlates with disease severity (Vanier 2010). Childhood onset of NP-C is most common, and based on "crowd-sourced" data, Bianconi et al. (2019) recently reported that NP-C patients have a median age of death at 13. There are limited disease-specific treatment options for NP-C, but none yet approved by the FDA (Hammond et al. 2019).

Previously, we reported metal dyshomeostasis in NP-C1 patient and mouse model plasma and various tissues including brain, liver and spleen (Hung et al. 2014). Dysregulated iron homeostasis is one of the key changes. Iron is significantly elevated in the brain (cerebellum and cerebrum) of BALB/cJ $Npc1^{nih}$ ($Npc1^{-/-}$) mice; and a trend to an increase in cerebellar iron in limited sample-size of post-mortem human NP-C1 cerebellar tissue. Brain iron elevation and disrupted iron metabolism increase adverse involvement of redox-active iron in Fenton or Haber-Weiss reactions, and thus promote oxidative stress by producing toxic levels of reactive oxygen species and free radicals. Oxidative stress is a pathological feature of NP-C (Reddy et al. 2006; Porter et al. 2010; Klein et al. 2011; Vazquez et al. 2011; Ribas et al. 2012; Vazquez et al. 2012), and abnormal iron metabolism may be a contributing factor.

Pathological brain iron accumulation has been identified as a potential therapeutic target for a number of neurodegenerative diseases that include Alzheimer's (AD) and Parkinson's (PD) diseases (Masaldan et al. 2019). Deferiprone (DFP), a brain penetrating iron chelator used to treat patients with iron overload disorders such as thalassemia, sickle cell anemia and hemochromatosis (Hider and Hoffbrand 2018; Fredenburg et al. 1996), is currently under investigation as a treatment option for AD and PD. DFP phase II clinical trials for PD (NCT00943748; NCT01539837) showed promising improvements in neurological outcomes and decreased nigral dentate and caudate nucleus iron levels (Martin-Bastida et al. 2017; Devos et al. 2014). Phase IIb clinical trials of DFP for PD are currently in progress (NCT02655315 and NCT02728843). Additionally, a phase II clinical trial of DFP for AD is underway (NCT03234686). Based on promising potential of DFP as a treatment option for AD and PD, we hypothesized that targeting brain iron accumulation in NP-C by iron chelation with DFP may improve neurological outcome and possibly lifespan in NP-C. To test this hypothesis, we investigated DFP treatment using the $Npc1^{nih}$ mouse model of NP-C.

Methods

Animals

This study used the BALB/cJ $Npc1^{nih}$ ($Npc1^{-/-}$) mouse model, a commonly used animal model of NP-C disease, which harbors *Npc1* null allele due to a spontaneous insertion mutation (Loftus et al. 1997). The $Npc1^{-/-}$ mice closely model the early childhood onset of the human NP-C disease, showing progressive weight loss, motor and cognitive impairments, and have a median lifespan of about 11 weeks (Maue et al. 2012; Voikar et al. 2002). Heterozygous $Npc1^{+/-}$ mice were used to generate $Npc1^{-/-}$ mice (n_{female} = 12; n_{male} = 12) used in this study. The $Npc1^{-/-}$ genotype was identified by real-time polymerase chain reaction with probes designed for *Npc1* (Transnetyx, Cordova, TN, USA). Mice were maintained at the Florey Core Animal Services Facility on Barastoc standard rodent feed (Ridley Corporation, Victoria,

Australia). Food and water were available *ad libitum*. After weaning at postnatal day (P) 21, male and female mice were housed separately, with a maximum of six mice of mixed genotype per cage, and maintained on a 12-h light-dark cycle.

Deferiprone treatment

DFP (3-hydroxy-1,2-dimethyl-4(1*H*)-pyridone; Sigma-Aldrich Cat #379409, Lot #STBG1231V) was dissolved using milliQ H_2O (Merck). Dissolved DFP was filter sterilized and warmed to 37 °C prior to use.

The *Npc1*$^{-/-}$ mice were assigned to four different treatment groups. They were assigned to start DFP treatment at two different ages: (1) pre-symptomatic (P15); and (2) symptomatic (P49). Within each of these groups, *Npc1*$^{-/-}$ mice were further assigned to be treated with (1) 75 mg/kg or (2) 150 mg/kg DFP. DFP treatment was administered by intraperitoneal (i.p.) injection three time a week (Monday, Wednesday and Friday). The choice of DFP dosage was based on previously reported DFP dosage for animal models of other neurological disorders, taking into consideration the young age of *Npc1*$^{-/-}$ mice (Ayton et al. 2013; Zhao et al. 2015; Devos et al. 2014).

Npc1$^{-/-}$ mice were weighed prior to receiving DFP by i.p. injection and for disease monitoring. The maximum injected volume of DFP was 1% of total body weight. Mice were sacrificed when they have lost $\geq$ 15% of their maximal body weight.

Experimental procedures were approved by the Florey Animal Ethics Committee and were conducted in accordance with the Australian Code for the Care and Use of Animals for Scientific Purposes, Eight Edition (2013).

Simon's two-stage design

Simon's two-stage design was used to assess the potential of DFP as a therapeutic drug for NP-C. Primary endpoint was extension of *Npc1*$^{-/-}$ mice lifespan by at least 50%, from expected median lifespan of 70 days to 105 days. An online calculator was used to generate Simon's two-stage design for this study: http://cancer.unc.edu/biostatistics/program/ivanova/SimonsTwoStageDesign.aspx. We tested the null hypothesis that the probability of DFP elicits a poor drug response is 5% against a one-sided alternative. In the first stage, enrolling $n_1 = 3$ *Npc1*$^{-/-}$ mice per experimental group. Within each experimental group, if none of the DFP-treated *Npc1*$^{-/-}$ mice survived to 105 days, the study will terminate. Otherwise, stage 2 will recruit additional $n_2 = 3$ *Npc1*$^{-/-}$ mice per experimental group to achieve a total of $n = 6$ *Npc1*$^{-/-}$ mice. The null hypothesis will be rejected if two or more mice survive for 105 days. This design yields a type I error rate of 2.66% and power of 82.8% when the response probability of DFP as an effective treatment is 50%.

Statistical analysis

Statistical analyses were performed using R version 3.4.3 (R Development Core Team 2017) and the following packages: cowplot (Wilke 2017), dplyr (Wickham et al. 2017), ggplot2 (Wickham 2009), ggpubr (Kassambara 2017), moments (Komsta and Novomestky 2015), rcompanion (Mangiafico 2018). To ensure satisfaction of distributional assumptions for statistical testing, the normality of data was checked visually by histogram and by Shapiro-Wilk test. Due to the small sample size, data that showed deviation from normal distribution were further tested for skewness. Data with a skewness value between -2 and 2 were considered to be within the acceptable range for normal distribution. Analysis of variance (ANOVA) and multiple comparisons of means [Tukey Honest Significant Difference test (TukeyHSD)] were used to assess differences in lifespan, onset of weight loss and onset of ataxia between the experimental groups. A one-sample Wilcoxon signed-rank test was used to compare the median lifespan of DFP-treated *Npc1*$^{-/-}$ mice against the expected median lifespan of 70 days (based on $\geq$15% loss of maximal body weight). The analyses also examined the interaction between sex, DFP start time, and DFP dose.

Results

To evaluate the potential of DFP as a treatment for NP-C, we treated commonly used *Npc1*^{nih} (*Npc1*$^{-/-}$) mouse model for NP-C with DFP in this study. To minimize the number of mice required for this evaluation, we adopted Simon's two-stage design for single-arm phase II clinical trials (Simon 1989), which allows for early termination of the study in the event

that DFP does not elicit positive improvements with respect to median lifespan as the primary endpoint. The expected median lifespan was 70 days (Hung et al. 2016), which was determined based on the criterion to sacrifice the mice when they have lost ≥ 15% of their maximal body weight.

Progressive weight loss is a part of the disease trajectory in the *Npc1*$^{-/-}$ mouse model. The onset of weight loss depended on the sex of *Npc1*$^{-/-}$ mice and their age at DFP treatment initiation (p = 0.0004; Fig. 1). There was no difference in the onset of weight loss between male and female *Npc1*$^{-/-}$ mice when DFP treatment began at P15. However, when DFP treatment begins at P49, the onset of weight loss was 7.3 days later in female *Npc1*$^{-/-}$ mice compared with male *Npc1*$^{-/-}$ mice. There was no difference in the onset of weight loss between the two doses tested.

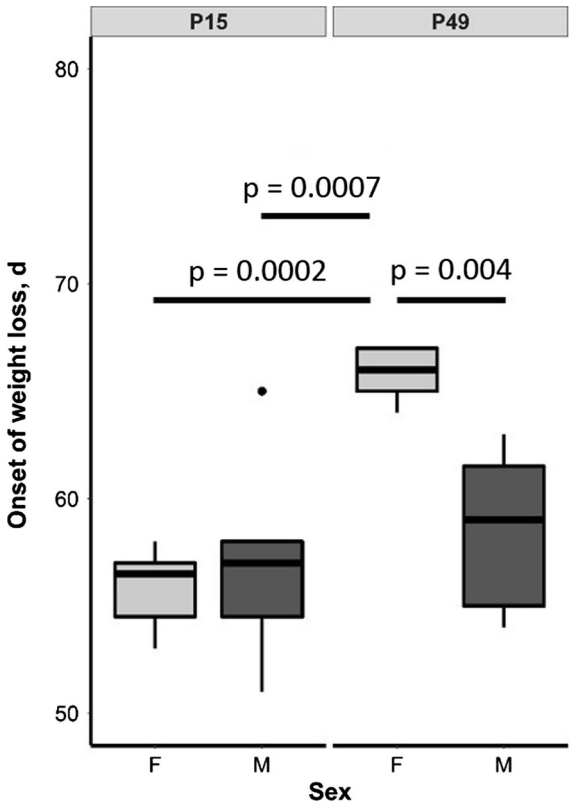

Fig. 1 The onset of weight loss in DFP-treated *Npc1*$^{-/-}$ mice depends on their sex and initiating age of DFP treatment. *Npc1*$^{-/-}$ mice were treated with 75 mg/kg or 150 mg/kg DFP, starting at P15 (pre-symptomatic) or P49 (symptomatic) three times a week (n = 3/sex/experimental group). The onset of weight loss occurred significantly later in female *Npc1*$^{-/-}$ mice that started DFP treatment at P49 compared with male mice and compared with mice that started DFP treatment at P15. Boxplot shows the median, the inter-quartile range (IQR), the highest and lowest values within 1.5 times the IQR, and outliers that lie more than 1.5 times the IQR. Statistical analysis: ANOVA followed by multiple pairwise comparison using Tukey HSD test.

Due to neurodegeneration of the cerebellum, *Npc1*$^{-/-}$ mice develop ataxia as the disease progresses. In this study, we visually monitored the onset of ataxia in *Npc1*$^{-/-}$ mice as a readout of their response to DFP treatment. Our analysis found an interaction between DFP dose and the sex of *Npc1*$^{-/-}$ mice (p = 0.02; Fig. 2a), and an interaction between DFP dose and age of DFP treatment initiation (p = 0.05; Fig. 2b). The onset of ataxia was observed eight days earlier in female *Npc1*$^{-/-}$ mice treated with 150 mg/kg DFP compared with those treated with 75 mg/kg DFP (Fig. 2a). There was no dose-dependent response observed for male *Npc1*$^{-/-}$ mice. For *Npc1*$^{-/-}$ mice that began DFP treatment at P15, the onset of ataxia began 7.9 days earlier in mice treated with 150 mg/kg DFP compared with those treated with 75 mg/kg (Fig. 2b). For *Npc1*$^{-/-}$ mice that began DFP treatment at P49, there was no dose-dependent onset of ataxia.

The expected median lifespan for *Npc1*$^{-/-}$ mice was 70 days. There was no difference in median lifespan of DFP-treated *Npc1*$^{-/-}$ mice with respect to their sex (Fig. 3a), age of DFP treatment initiation (Fig. 3b), or DFP dose (Fig. 3c). There was no change in the median lifespan of DFP-treated *Npc1*$^{-/-}$ mice compared with the expected median lifespan (p = 0.77). As none of the *Npc1*$^{-/-}$ mice survived longer than the expected median lifespan of 70 days, the study was terminated at the end of stage 1 based on our pre-determined criteria for Simon's two-stage design.

Discussion

Previously, our metallomic analysis revealed significantly elevated brain iron in *Npc1*$^{-/-}$ mice and a trend to increased cerebellar iron in post-mortem human NP-C brain (Hung et al. 2014). We hypothesized that, similar to abnormal iron accumulation in AD and PD, this increase in NP-C brain iron may contribute to disease pathogenesis, and in particular, the underlying

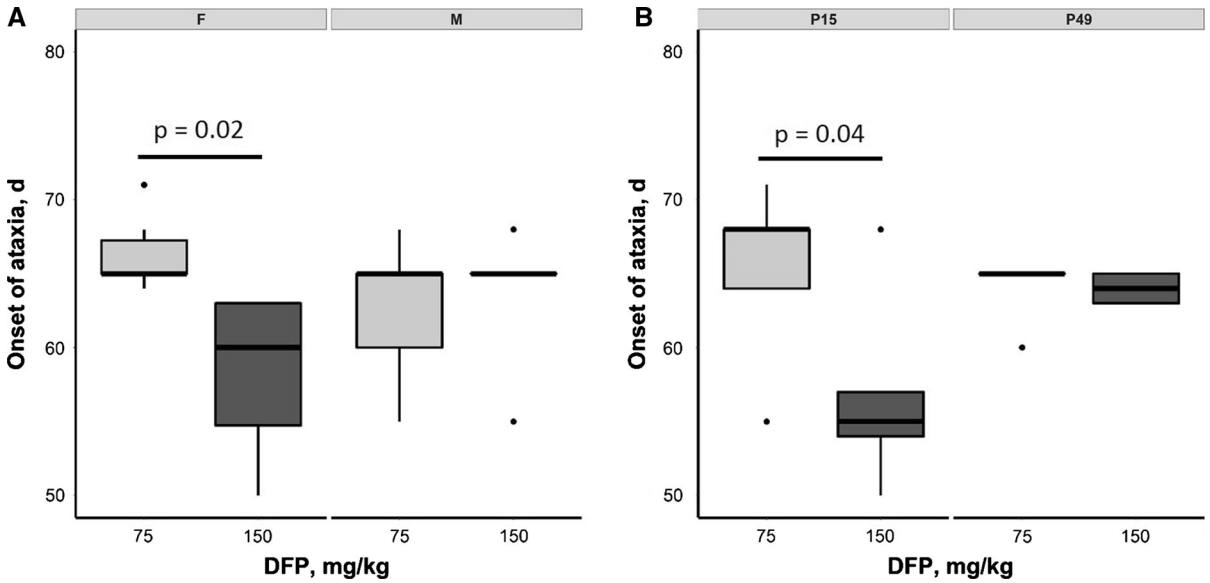

Fig. 2 The onset of ataxia in DFP-treated *Npc1*$^{-/-}$ depends on the dose administered, but the time of onset also varies according to their sex (**a**) and differs depending on the initiating age of DFP treatment (**b**). *Npc1*$^{-/-}$ mice were treated with 75 mg/kg or 150 mg/kg DFP, starting at P15 (pre-symptomatic) or P49 (symptomatic) three times a week (n = 3/sex/experimental group). Boxplot shows the median, the inter-quartile range (IQR), the highest and lowest values within 1.5 times the IQR, and outliers that lie more than 1.5 times the IQR. Statistical analysis: ANOVA followed by multiple pairwise comparison using Tukey HSD test.

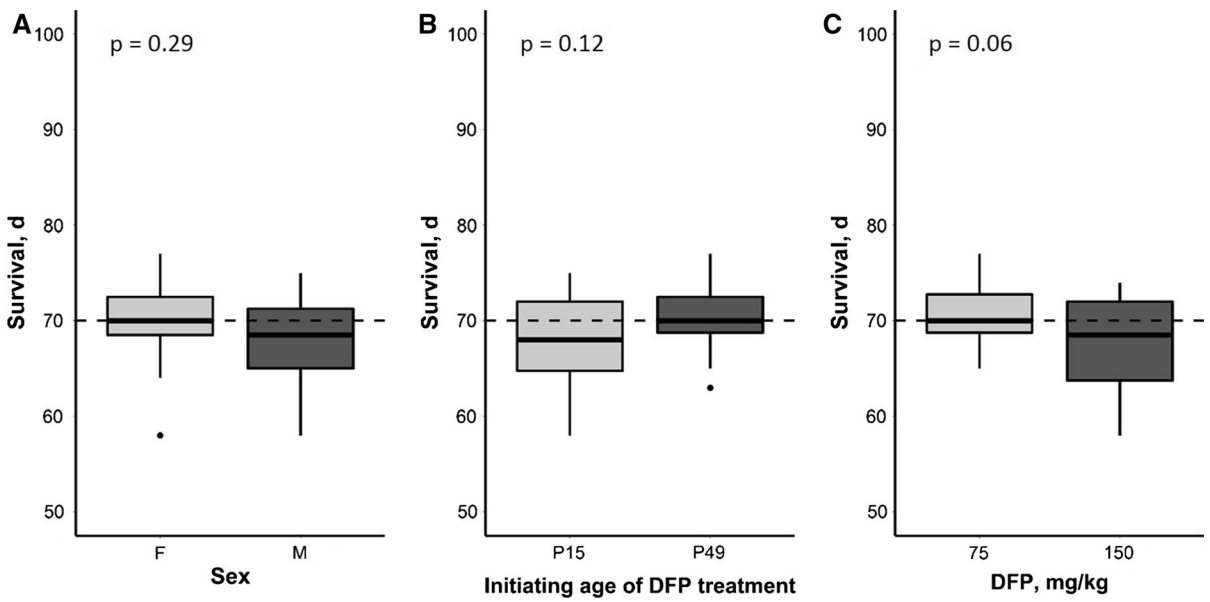

Fig. 3 DFP treatment did not improve the lifespan of *Npc1*$^{-/-}$ mice. Compared against the expected median lifespan of 70 days (indicated by the dashed line), there was no change in *Npc1*$^{-/-}$ mice lifespan or between sex groups (**a**), different initiating age of DFP treatment (**b**), and DFP doses (**c**). *Npc1*$^{-/-}$ mice were treated with 75 mg/kg or 150 mg/kg DFP, starting at P15 (pre-symptomatic) or P49 (symptomatic) three times a week (n = 3/sex/experimental group). Boxplot shows the median, the inter-quartile range (IQR), the highest and lowest values within 1.5 times the IQR, and outliers that lie more than 1.5 times the IQR. Statistical analysis: ANOVA followed by multiple pairwise comparison using Tukey HSD test.

oxidative stress by promoting Fenton and/or Haber-Weiss reactions. Iron chelation therapy with DFP has demonstrated neuroprotective effects and improved motor and cognitive outcomes in PD (Devos et al. 2014; Martin-Bastida et al. 2017) and are in further phase II clinical trials for PD (NCT02655315 and NCT02728843) and AD (NCT03234686). Therefore, we hypothesized that iron chelation therapy with DFP, targeting the abnormal brain iron accumulation in NP-C, may elicit similar neuroprotective therapeutic benefits. However, contrary to our expectations, DFP was ineffective in slowing the disease progression or prolong the lifespan of *Npc1*$^{-/-}$ mice. Moreover, our results showed that higher dose of DFP and initiating treatment at an earlier age (P15) resulted in increased toxicity.

The ineffectiveness of DFP in treating *Npc1*$^{-/-}$ mice in this study may be attributed a combination of significantly decreased hepatic iron levels in *Npc1*$^{-/-}$ mice (Hung et al. 2014) and administration of DFP by i.p. injection. DFP is orally bioavailable and many studies administer DFP in drinking water (Carboni et al. 2017; Casu et al. 2016; Zhao et al. 2015; Ayton et al. 2013). However, voluntary consumption may be variable between animals and produce confounding results. To ensure precise and accurate oral dosing, the preferred method is oral gavage. It is possible to give oral gavage to pre-weaning and young mice (Moser et al. 2005), but repeated dosing required by this study risks damage to the thin esophageal tissues of young animals used. Consequently, we chose to administer DFP by i.p. injections based on similarity in pharmacokinetics between this delivery route and that of oral administration (Turner et al. 2011). Absorption of drugs delivered by i.p. occurs primarily through portal circulation and can thus undergo hepatic metabolism before systemic distribution (Lukas et al. 1971). The detrimental effect of DFP treatment found in this study may be the result of DFP further depleting the already deficient hepatic iron content in *Npc1*$^{-/-}$ mice.

Another explanation for the negative outcome of iron chelation therapy with DFP in *Npc1*$^{-/-}$ mice is the potential detrimental effects exerted by lowering brain iron during sensitive neurodevelopmental periods. In healthy human brain, high levels of iron accumulates in the basal ganglia with age (Ramos et al. 2014). Age-related iron accumulation may contribute to neurotoxicity and consequently, apoptosis and ferroptosis that result in neurodegeneration (Masaldan et al. 2019). For late life neurodegenerative disorders such as AD and PD, where age-related iron accumulation and compromised brain iron metabolism have been implicated in disease pathogenesis, removal of excess iron by iron chelation therapy resulted in neurological improvements (Devos et al. 2014; Martin-Bastida et al. 2017). In this study, the age of iron chelation treatment with DFP for *Npc1*$^{-/-}$ mice began at P15 and P49, which are equivalent to human age of about 3 months and 13.4 years old, respectively (Dutta and Sengupta 2016). Iron is critical to brain development and in particular, the rapid axon myelination during these developmental periods (Snaidero and Simons 2014; Wessling-Resnick 2017). Optimal brain development requires balanced iron levels; iron deficiency or overload would result in neurological deficits. The brain iron elevation in *Npc1*$^{-/-}$ mice may represent greater iron influx due to *Npc1* deficiency and/or greater need for iron that remains to be determined. This scenario could be similar to the accumulation of iron in Friedreich's ataxia caused by mutation of frataxin, where defects in the transfer of iron to iron-sulfur clusters (ISCs) leads to both a metabolic deficiency of ISCs as well as an upstream toxic build-up of iron (Ast et al. 2019). The increase in brain iron in *Npc1*$^{-/-}$ mice may contribute to their neurological phenotype, but the concentration may not have reached the same neurotoxic level as in old age. It is possible that the DFP doses used in this study may have caused excessive iron depletion, rather than restore the iron homeostasis and facilitate neuroprotection.

In conclusion, our pilot study showed that in a relevant mouse model of NP-C, targeting brain iron accumulation in early life is ineffective and potentially harmful. These findings may bear implications for other rare genetic childhood-onset disorders manifesting as Neurodegeneration with Brain Iron Accumulation (NBIAs), in which iron chelation, although potentially effective (Klopstock et al. 2019), must be considered with care to avoid over depletion of iron critical to brain development.

Acknowledgements The authors wish to thank Dr. Ibrahima Diouf for statistical advice. This work was supported by research grants from the Australian NPC Disease Foundation, Inc. to Y.H.H. and A.I.B.; the Australia-Israel Medical Research Foundation (AUSiMED) to A.L. and A.I.B.; Victoria Israel Science Innovation and Technology Scheme Grants for Feasibility and Proof of Concept Projects to A.L. and A.I.B.;

Cooperative Research Centre for Mental Health to A.I.B. The Florey Institute of Neuroscience and Mental Health acknowledges the strong support of the Victorian Government and in particular funding from the Operational Infrastructure Support Grant.

Author contributions A.I.B. and A.L. conceived the idea for this study. Y.H.H. and A.L. designed and planned the experiments, and performed data analysis. A.S. and S.Y. performed the experiments and contributed to interpretation of results. Y.H.H. wrote the manuscript with inputs from all authors.

Funding This work was supported by research grants from the Australian NPC Disease Foundation, Inc.; the Australia-Israel Medical Research Foundation (AUSiMED); Victoria Israel Science Innovation and Technology Scheme Grants for Feasibility and Proof of Concept Projects; Cooperative Research Centre for Mental Health; and the Victorian Government Operational Infrastructure Support Grant

Compliance with ethical standards

Conflict of interest A.I.B. is a shareholder of Prana Biotechnology Ltd, Cogstate Ltd, Brighton Biotech LLC, Grunbiotics Pty Ltd, Eucalyptus Pty Ltd, and Mesoblast Ltd. He is a paid consultant for, and has a profit share interest in Collaborative Medicinal Development LLC.

Ethical approval Animal experimental procedures were approved by the Florey Animal Ethics Committee (AEC# 17–042).

References

Ast T, Meisel JD, Patra S, Wang H, Grange RMH, Kim SH, Calvo SE, Orefice LL, Nagashima F, Ichinose F, Zapol WM, Ruvkun G, Barondeau DP, Mootha VK (2019) Hypoxia rescues Frataxin loss by restoring iron sulfur cluster biogenesis. Cell 177:1507–1528

Ayton S, Lei P, Duce JA, Wong BX, Sedjahtera A, Adlard PA, Bush AI, Finkelstein DI (2013) Ceruloplasmin dysfunction and therapeutic potential for Parkinson disease. Ann Neurol 73:554–559

Bianconi SE, Hammond DI, Farhat NY, Dang Do A, Jenkins K, Cougnoux A, Martin K, Porter FD (2019) Evaluation of age of death in Niemann-Pick disease, type C: utility of disease support group websites to understand natural history. Mol Genet Metab 126:466–469

Carboni E, Tatenhorst L, Tonges L, Barski E, Dambeck V, Bahr M, Lingor P (2017) Deferiprone rescues behavioral deficits induced by mild iron exposure in a mouse model of alpha-Synuclein aggregation. Neuromolecular Med 19:309–321

Carstea ED, Morris JA, Coleman KG, Loftus SK, Zhang D, Cummings C, Gu J, Rosenfeld MA, Pavan WJ, Krizman DB, Nagle J, Polymeropoulos MH, Sturley SL, Ioannou YA, Higgins ME, Comly M, Cooney A, Brown A, Kaneski CR, Blanchette-Mackie EJ, Dwyer NK, Neufeld EB, Chang TY, Liscum L, Strauss JF, Ohno K, Zeigler M, Carmi R, Sokol J, Markie D, O'Neill RR, van Diggelen OP, Elleder M, Patterson MC, Brady RO, Vanier MT, Pentchev PG, Tagle DA (1997) Niemann-Pick C1 disease gene: homology to mediators of cholesterol homeostasis. Science 277:228–231

Casu C, Oikonomidou PR, Chen H, Nandi V, Ginzburg Y, Prasad P, Fleming RE, Shah YM, Valore EV, Nemeth E, Ganz T, MacDonald B, Rivella S (2016) Minihepcidin peptides as disease modifiers in mice affected by beta-thalassemia and polycythemia vera. Blood 128:265–76

Devos D, Moreau C, Devedjian JC, Kluza J, Petrault M, Laloux C, Jonneaux A, Ryckewaert G, Garcon G, Rouaix N, Duhamel A, Jissendi P, Dujardin K, Auger F, Ravasi L, Hopes L, Grolez G, Firdaus W, Sablonniere B, Strubi-Vuillaume I, Zahr N, Destee A, Corvol JC, Poltl D, Leist M, Rose C, Defebvre L, Marchetti P, Cabantchik ZI, Bordet R (2014) Targeting chelatable iron as a therapeutic modality in Parkinson's disease. Antioxid Redox Signal 21:195–210

Dutta S, Sengupta P (2016) Men and mice: relating their ages. Life Sci 152:244–248

Elghobashi-Meinhardt N (2019) Computational tools unravel putative sterol binding sites in the lysosomal NPC1 protein. J Chem Inf Model 59:2432–2441

Fredenburg AM, Sethi RK, Allen DD, Yokel RA (1996) The pharmacokinetics and blood-brain barrier permeation of the chelators 1,2 dimethly-, 1,2 diethyl-, and 1-[ethan-1'ol]-2-methyl-3-hydroxypyridin-4-one in the rat. Toxicology 108:191–199

Gong X, Qian H, Zhou X, Wu J, Wan T, Cao P, Huang W, Zhao X, Wang X, Wang P, Shi Y, Gao GF, Zhou Q, Yan N (2016) Structural insights into the Niemann-Pick C1 (NPC1)-mediated cholesterol transfer and ebola infection. Cell 165:1467–1478

Hammond N, Munkacsi AB, Sturley SL (2019) The complexity of a monogenic neurodegenerative disease: more than two decades of therapeutic driven research into Niemann-Pick type C disease. Biochim Biophys Acta 1864:1109–1123

Hider RC, Hoffbrand AV (2018) The role of deferiprone in iron chelation. N Engl J Med 379:2140–2150

Hodoscek M, Elghobashi-Meinhardt N (2018) Simulations of NPC1(NTD):NPC2 protein complex reveal cholesterol transfer pathways. Int J Mol Sci 19:E2623

Hung YH, Faux NG, Killilea DW, Yanjanin N, Firnkes S, Volitakis I, Ganio G, Walterfang M, Hastings C, Porter FD, Ory DS, Bush AI (2014) Altered transition metal homeostasis in Niemann-Pick disease, type C1. Metallomics 6:542–53

Hung YH, Walterfang M, Churilov L, Bray L, Jacobson LH, Barnham KJ, Jones NC, O'Brien TJ, Velakoulis D, Bush AI (2016) Neurological dysfunction in early maturity of a model for Niemann-Pick C1 carrier status. Neurotherapeutics 13:614–22

Kassambara A (2017) ggpubr: 'ggplot2' based publication ready plots. R package version 0.1.6

Klein A, Maldonado C, Vargas LM, Gonzalez M, Robledo F, Perez de Arce K, Munoz FJ, Hetz C, Alvarez AR, Zanlungo S (2011) Oxidative stress activates the c-Abl/p73 proapoptotic pathway in Niemann-Pick type C neurons. Neurobiol Dis 41:209–218

Klopstock T, Tricta F, Neumayr L, Karin I, Zorzi G, Fradette C, Kmiec T, Buchner B, Steele HE, Horvath R, Chinnery PF, Basu A, Kupper C, Neuhofer C, Kalman B, Dusek P, Yapici Z, Wilson I, Zhao F, Zibordi F, Nardocci N, Aguilar C, Hayflick SJ, Spino M, Blamire AM, Hogarth P, Vichinsky E (2019) Safety and efficacy of deferiprone for pantothenate kinase-associated neurodegeneration: a randomised, double-blind, controlled trial and an open-label extension study. Lancet Neurol 18:631–642

Komsta L, Novomestky F (2015) moments: moments, cumulants, skewness, kurtosis and related tests. R package version 0.14

Li X, Lu F, Trinh MN, Schmiege P, Seemann J, Wang J, Blobel G (2017) 3.3 A structure of Niemann-Pick C1 protein reveals insights into the function of the C-terminal luminal domain in cholesterol transport. Proc Natl Acad Sci USA 114:9116–9121

Loftus SK, Morris JA, Carstea ED, Gu JZ, Cummings C, Brown A, Ellison J, Ohno K, Rosenfeld MA, Tagle DA, Pentchev PG, Pavan WJ (1997) Murine model of Niemann-Pick C disease: mutation in a cholesterol homeostasis gene. Science 277:232–235

Lukas G, Brindle SD, Greengard P (1971) The route of absorption of intraperitoneally administered compounds. J Pharmacol Exp Ther 178:562–564

Mangiafico S (2018) rcompanion: functions to support extension education program evaluation. R package version 1.11.3

Martin-Bastida A, Ward RJ, Newbould R, Piccini P, Sharp D, Kabba C, Patel MC, Spino M, Connelly J, Tricta F, Crichton RR, Dexter DT (2017) Brain iron chelation by deferiprone in a phase 2 randomised double-blinded placebo controlled clinical trial in Parkinson's disease. Sci Rep 7:1398

Masaldan S, Bush AI, Devos D, Rolland AS, Moreau C (2019) Striking while the iron is hot: Iron metabolism and ferroptosis in neurodegeneration. Free Radic Biol Med 133:221–233

Maue RA, Burgess RW, Wang B, Wooley CM, Seburn KL, Vanier MT, Rogers MA, Chang CC, Chang TY, Harris BT, Graber DJ, Penatti CA, Porter DM, Szwergold BS, Henderson LP, Totenhagen JW, Trouard TP, Borbon IA, Erickson RP (2012) A novel mouse model of Niemann-Pick type C disease carrying a D1005G-Npc1 mutation comparable to commonly observed human mutations. Hum Mol Genet 21:730–50

Moser VC, Walls I, Zoetis T (2005) Direct dosing of preweaning rodents in toxicity testing and research: deliberations of an ILSI RSI Expert Working Group. Int J Toxicol 24:87–94

Naureckiene S, Sleat DE, Lackland H, Fensom A, Vanier MT, Wattiaux R, Jadot M, Lobel P (2000) Identification of HE1 as the second gene of Niemann-Pick C disease. Science 290:2298–2301

Patterson MC, Mengel E, Wijburg FA, Muller A, Schwierin B, Drevon H, Vanier MT, Pineda M (2013) Disease and patient characteristics in NP-C patients: findings from an international disease registry. Orphanet J Rare Dis 8:12

Pfeffer SR (2019) NPC intracellular cholesterol transporter 1 (NPC1)-mediated cholesterol export from lysosomes. J Biol Chem 294:1706–1709

R Development Core Team (2017) R: a language and environment for statistical computing. R Foundation for Statistical Computing, Vienna

Porter FD, Scherrer DE, Lanier MH, Langmade SJ, Molugu V, Gale SE, Olzeski D, Sidhu R, Dietzen DJ, Fu R, Wassif CA, Yanjanin NM, Marso SP, House J, Vite C, Schaffer JE, Ory DS (2010) Cholesterol oxidation products are sensitive and specific blood-based biomarkers for Niemann-Pick C1 disease. Sci Transl Med 2:56ra81

Ramos P, Santos A, Pinto NR, Mendes R, Magalhaes T, Almeida A (2014) Iron levels in the human brain: a post-mortem study of anatomical region differences and age-related changes. J Trace Elem Med Biol 28:13–17

Reddy JV, Ganley IG, Pfeffer SR (2006) Clues to neuro-degeneration in Niemann-Pick type C disease from global gene expression profiling. PLoS ONE 1:e19

Rego T, Farrand S, Goh AMY, Eratne D, Kelso W, Mangelsdorf S, Velakoulis D, Walterfang M (2019) Psychiatric and cognitive symptoms associated with Niemann-Pick type c disease: neurobiology and management. CNS Drugs 33(2):125–142

Ribas GS, Pires R, Coelho JC, Rodrigues D, Mescka CP, Vanzin CS, Biancini GB, Negretto G, Wayhs CA, Wajner M, Vargas CR (2012) Oxidative stress in Niemann-Pick type C patients: a protective role of *N*-butyl-deoxynojirimycin therapy. Int J Dev Neurosci 30:439–444

Simon R (1989) Optimal two-stage designs for phase II clinical trials. Control Clin Trials 10:1–10

Snaidero N, Simons M (2014) Myelination at a glance. J Cell Sci 127:2999–3004

Turner PV, Brabb T, Pekow C, Vasbinder MA (2011) Administration of substances to laboratory animals: routes of administration and factors to consider. J Am Assoc Lab Anim Sci 50:600–613

Vanier MT (2010) Niemann-Pick disease type C. Orphanet J Rare Dis 5:16

Vazquez MC, del Pozo T, Robledo FA, Carrasco G, Pavez L, Olivares F, Gonzalez M, Zanlungo S (2011) Alteration of gene expression profile in Niemann-Pick type C mice correlates with tissue damage and oxidative stress. PLoS ONE 6:e28777

Vazquez MC, Balboa E, Alvarez AR, Zanlungo S (2012) Oxidative stress: a pathogenic mechanism for Niemann-Pick type C disease. Oxid Med Cell Longev 2012:205713

Voikar V, Rauvala H, Ikonen E (2002) Cognitive deficit and development of motor impairment in a mouse model of Niemann-Pick type C disease. Behav Brain Res 132:1–10

Wassif CA, Cross JL, Iben J, Sanchez-Pulido L, Cougnoux A, Platt FM, Ory DS, Ponting CP, Bailey-Wilson JE, Biesecker LG, Porter FD (2016) High incidence of unrecognized visceral/neurological late-onset Niemann-Pick disease, type C1, predicted by analysis of massively parallel sequencing data sets. Genet Med 18:41–48

Wessling-Resnick M (2017) Excess iron: considerations related to development and early growth. Am J Clin Nutr 106:1600S-1600S05S

Wickham H (2009) ggplot2: elegant graphics for data analysis. Springer, Berlin

Wickham H, Francois R, Henry L, Kirill M (2017) dplyr: a grammar of data manipulation. R package version 0.7.4

Wilke CO (2017) Cowplot: streamlined plot theme and plot annotations for 'ggplot2'. R package version 0.9.2

Xu S, Benoff B, Liou HL, Lobel P, Stock AM (2007) Structural basis of sterol binding by NPC2, a lysosomal protein deficient in Niemann-Pick type C2 disease. J Biol Chem 282:23525–23531

Zhao L, Hadziahmetovic M, Wang C, Xu X, Song Y, Jinnah HA, Wodzinska J, Iacovelli J, Wolkow N, Krajacic P, Weissberger AC, Connelly J, Spino M, Lee MK, Connor J, Giasson B, Harris ZL, Dunaief JL (2015) Cp/Heph mutant mice have iron-induced neurodegeneration diminished by deferiprone. J Neurochem 135:958–974